MAGNETOSOME DYNAMICS IN MAGNETOTACTIC BACTERIA

S. OFER†, I. NOWIK, AND E. R. BAUMINGER
Racah Institute of Physics, Hebrew University, Jerusalem, Israel

G. C. PAPAEFTHYMIOU AND R. B. FRANKEL
Francis Bitter National Magnet Laboratory, Massachusetts Institute of Technology, Cambridge, Massachusetts 02139

R. P. BLAKEMORE
Department of Microbiology, University of New Hampshire, Durham, New Hampshire 03424

ABSTRACT Diffusive motions of the magnetosomes (enveloped Fe_3O_4 particles) in the magnetotactic bacterium *Aquaspirillum magnetotacticum* result in a very broad-line Mössbauer spectrum ($\Gamma \sim 100$ mm/s) above freezing temperatures. The line width increases with increasing temperature. The data are analyzed using a bounded diffusion model to yield the rotational and translational motions of the magnetosomes as well as the effective viscosity of the material surrounding the magnetosomes. The results are $\langle\theta^2\rangle^{1/2} < 1.5°$ and $\langle x^2\rangle^{1/2} < 8.4$ Å for the rotational and translational motions, respectively, implying that the particles are fixed in whole cells. The effective viscosity is 10 cP at 295 K and increases with decreasing temperature. Additional Fe^{3+} material in the cell is shown to be associated with the magnetosomes. Fe^{2+} material in the cell appears to be associated with the cell envelope.

INTRODUCTION

Iron accounts for 2% of the dry weight of the magnetotactic bacterium *Aquaspirillum magnetotacticum* (1). Most of the iron (80–90%) is present in the form of intracytoplasmic, enveloped, 40–50 nm wide particles of Fe_3O_4 (2, 3). Cells also contain ferrous iron and hydrous-ferric-oxide (ferrihydrite) (4). The enveloped Fe_3O_4 particles, which are termed magnetosomes (3), are arranged in a chain that longitudinally traverses the cell in close proximity to the inner surface of the cytoplasmic membrane (3). The number of magnetosomes in the chain is variable, depending upon the culture conditions, but typically averages 20. Magnetosomes are enveloped by electron-transparent and electron-dense layers and each is separated from those adjacent to it by 10 nm regions containing cytoplasmic material free of ribosomes or other particulate elements (3). The chemical composition of the distinctive region surrounding bacterial magnetite grains is unknown but may be important in their formation. Magnetite particles extracted from cells by brief sonication retain an envelope although their interparticle separation is <50% of that separating particles in chains within intact cells (3).

The magnetosomes impart a magnetic dipole moment to the cell, parallel to the axis of motility (2). According to the passive orientation hypothesis (5), the cell is oriented as it swims in the geomagnetic field by the torque exerted on the magnetic dipole moment by the field. The fact that the entire bacterium is oriented implies that the motions of the individual particles relative to each other are small and that the effective viscosity of the magnetosome surroundings in the cell is high compared with the viscosity of water; otherwise, the magnetic dipole moment of the cell could change its orientation with respect to the axis of motility. However, until now there has been no way to determine the motions of the magnetosomes in the cells.

In this paper we report that Mössbauer spectroscopy of whole cells above the freezing point of water can be used to measure the motions of the magnetosomes and to determine the effective viscosity of the magnetosome surroundings. The determination is based on the fact that in cells at ambient temperatures the magnetosomes will undergo small diffusive displacements, the magnitude of which are related to the viscosity of their surroundings. It has been previously shown that for iron containing colloidal particles introduced into a viscous fluid, the Mössbauer line width is inversely proportional to the viscosity of the fluid (6). Furthermore, it has been demonstrated recently that the Mössbauer effect (ME) on iron-containing proteins in cells can be used to determine the viscosity of the iron containing environment (7).

In the present case, Mössbauer measurements were performed between 90 and 295 K on packed cells *A. magnetotacticum*, which were cultured in chemically

†Deceased.

defined media containing ferric quinate enriched in Fe^{57} (the Mössbauer sensitive isotope). The spectra were analyzed using a bounded diffusion model derived below. We find that rotational and translational motions of the individual particles are small ($\langle\theta^2\rangle^{1/2} < 1.5°$; $\langle x^2\rangle^{1/2} < 8.4$ Å) and that the effective viscosity of the cytoplasm of the magnetotactic bacteria is ~15 times greater than the viscosity of water.

In addition, the results give information about the location of the other iron-containing materials, precursors to Fe_3O_4 precipitation (4), in the cells. The hydrous-ferric-oxide is associated with the magnetosomes, whereas the Fe^{2+} is localized elsewhere in the cell, possibly in the cell envelope.

METHODS

Organism and Culture Conditions

A. magnetotacticum strain MS-1 was used throughout (8). Cells enriched in Fe-57 were cultured microaerobically on a chemically defined medium as described previously (1). The medium contained tartaric and succinic acids as carbon sources, ferric quinate as the principal iron source and sodium nitrate, ammonium sulfate, or a combination as the nitrogen source. Cells were grown in 10-liter glass carboys to late logarithmic or early stationary phase (10–14 d; 2.0×10^8 cells/ml, at 30°C). They were harvested by continuous-flow centrifugation in an electrically driven centrifuge equipped with water cooling. The cells were washed twice at 5°C in 10–20 ml of cold 50 mM potassium phosphate buffer (pH 6.9) and centrifuged into a pellet with the consistency of paste. The wet cell material was packed into 1 ml plastic Mössbauer absorber cells with tight-fitting covers. These Mössbauer samples were either frozen and subsequently analyzed, or, in one case, analyzed immediately without freezing. The experimental spectra were found to be independent of whether the cells were frozen at the end or the beginning of the series of measurements, and except for measurements close to the freezing point, showed no temperature hysteresis.

$^{57}FeCl_3$ was prepared by first dissolving 80 mg Fe_2O_3, isotopically enriched to 90% ^{57}Fe, in 4.5 ml analytical grade concentrated HCl. Excess HCl was then boiled off to concentrate the resulting $FeCl_3$ to a sample volume of 1 ml. The concentrate was diluted with 5–10 ml distilled H_2O and again concentrated by boiling. This procedure was repeated two more times and the $^{57}FeCl_3$ was finally taken to near dryness. The salt was then dissolved in 100 ml distilled H_2O and combined with 0.19 *g D*-quinic acid (Sigma Chemical Co., St. Louis, MO) to chelate the metal. 20 ml of this 0.01 M stock of ferric quinate, sterilized by autoclaving, was asceptically added to each 10 liters of medium prior to inoculation.

Mössbauer Spectroscopy

Mössbauer measurements were performed using a conventional, constant acceleration spectrometer, with velocities extending up to ± 100 mm/s. A 100 mCi source of Co^{57} in Rh was maintained at room temperature. The absorber consisting of packed cells was held in a cryostat in helium vapor. Measurements between 90 and 295 K were carried out with the temperature stabilized to within 0.1 K. The spectra were least-squares fitted by computer, assuming Lorentzian line shapes.

EXPERIMENTAL RESULTS

The Mössbauer spectrum of whole packed cells at $T < 265$ K consisted primarily of the spectrum due to Fe_3O_4 (Fig. 1) (4). The spectrum consists of sharp, magnetic hyperfine lines between approximately +8 and −8 mm/s. Six lines

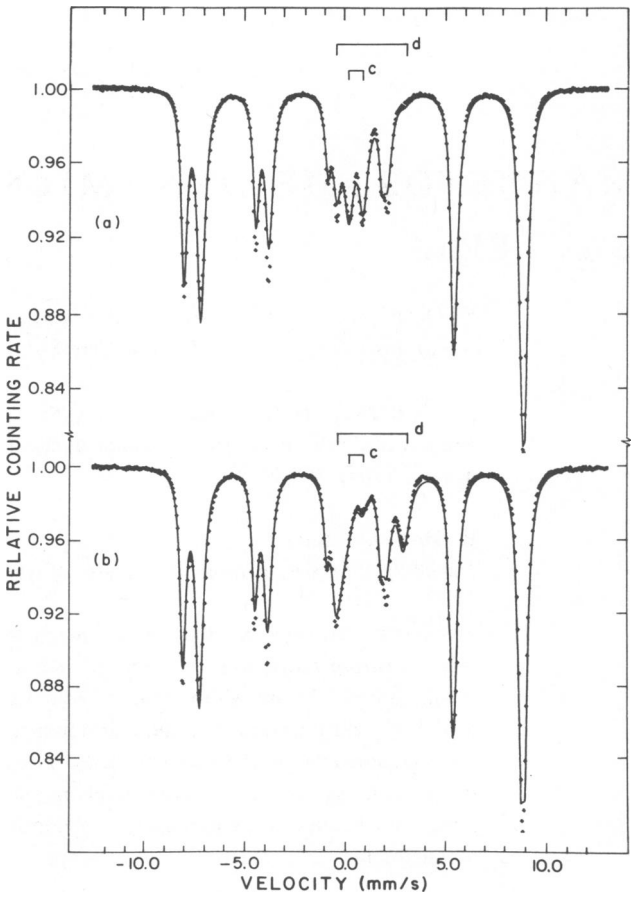

FIGURE 1 Mössbauer spectra of magnetotactic bacteria at 200 K. (*a*) The spectrum of a sample frozen immediately after harvesting the cells. (*b*) The spectrum obtained in a sample which was held above 285 K for a few days before freezing. Lines at position *c* correspond to an Fe^{3+} quadrupole doublet. Lines at position *d* correspond to an Fe^{2+} doublet. The solid lines are least squares computer fits to the experimental spectra.

are due to Fe^{3+} in tetrahedral sites and six lines are due to Fe^{3+} and Fe^{2+} in octahedral sites. The two highest velocity lines of the tetrahedral and octahedral site spectra fortuitously superpose giving 10 resolvable lines. There is no discernible absorption for velocities greater than ~8 mm/s and less then −8 mm/s. In samples kept frozen after collection of the bacteria, there were two additional quadrupole doublets (Fig. 1 *a*). One doublet, with intensity corresponding to ~13% of the total iron, had parameters typical of Fe^{3+} (isomer shift relative to iron metal $\delta = 0.42 \pm 0.02$ mm/s; quadrupole splitting $\Delta E_Q = 0.63 \pm 0.02$ mm/s). The other doublet, with intensity corresponding to <2% of total iron, had parameters typical of Fe^{2+} ($\delta = 1.12 \pm 0.02$ mm/s; $\Delta E_Q = 2.88 \pm 0.02$ mm/s). These doublets have been ascribed to precursors in the biomineralization of Fe_3O_4 in the bacteria (4). When the cells were held above 280 K in the sealed container for several days and refrozen, the Fe_3O_4 spectrum was unchanged, but the intensities of the two doublets had reversed, indicating that the Fe^{3+} material in the cell had been reduced to Fe^{2+} (Fig. 1 *b*).

The Mössbauer spectrum of the whole cells at $T > 275$ K was dramatically different from that of the frozen cells ($T < 265$ K) (Fig. 2). At 275 K it consisted primarily of a broad line of width $\Gamma = 72 \pm 1$ mm/s. The width of the broad line increased with increasing temperature to $\Gamma = 139$ mm/s at $T = 295$ K (Fig. 3). However, the total spectral intensity was temperature independent and equal to the total spectral intensity of the sharp line spectrum of the frozen cells (Fig. 4). Some hysteresis in the solid-liquid transition was noted in spectra obtained at 270 K. If the sample temperature had been increased from 265 K, the sharp-line spectrum was observed. However, if the sample temperature had been decreased from 275 K the broad line spectrum was obtained. For $T > 275$ K, computer analysis showed that the intensity of the sharp-line Fe_3O_4 spectrum superposed on the broad line spectrum was <0.2%.

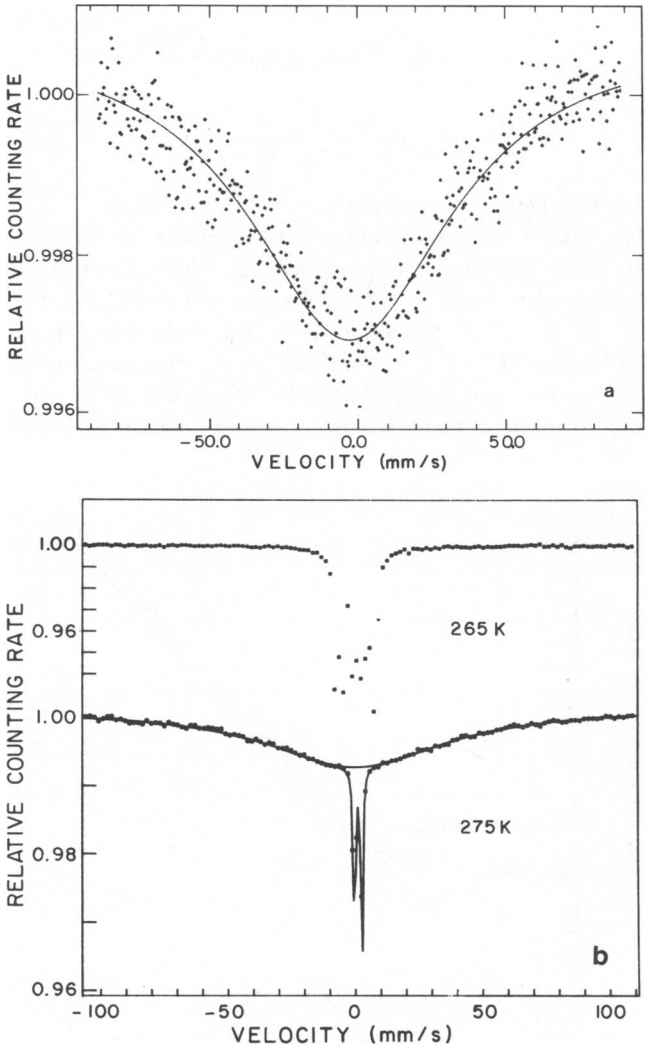

FIGURE 2 (*a*) Mössbauer spectrum at 275 K of the sample corresponding to the spectrum in Fig. 1 *a*. The width of the broad line is the same as in *b* (275 K). There is no superposed sharp-line spectrum due to Fe^{3+}. (*b*) Mössbauer spectra obtained at 265 K and 275 K of the sample corresponding to the spectrum in Fig. 1 *b*. The spectrum at 265 K is very similar to that at 200 K, but is shown here on an extended velocity scale. Only the experimental points are shown in this spectrum. The solid line in the 275 K spectrum is a least squares computer fit to the experimental points, consisting of a wide line of width (72 ± 1) mm/s and a well-defined doublet of small relative intensity, corresponding to Fe^{2+}.

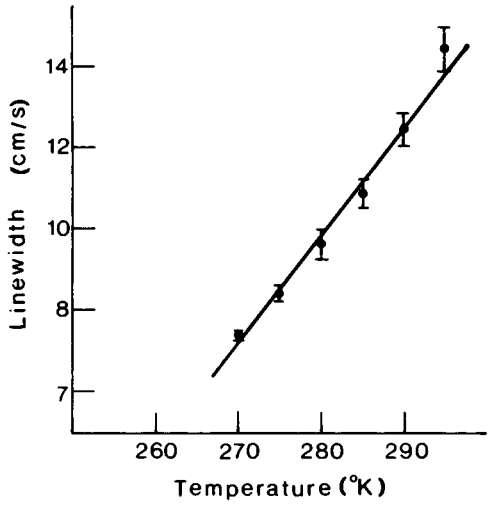

FIGURE 3 The line width of the broad line in the Mössbauer spectra plotted as function of temperature. Note units in centimeters per second on the ordinate.

The temperature dependence of the additional quadrupole doublet depended on whether the iron was primarily Fe^{3+} or Fe^{2+}. When the additional iron was Fe^{3+}, as evidenced by the parameters of the doublet in the $T = 265$ K spectrum, there was no residual doublet superposed on the broad-line spectrum at $T \geq 275$ K. However, when the additional iron was primarily Fe^{2+}, the low intensity, sharp line Fe^{2+} doublet remained superposed on the broad-line spectrum (Fig. 2 *b*).

The dramatic change of the spectral shape from a normal sharp-line spectrum between −8 and +8 mm/s to an extremely broad-line spectrum with width of ~100 mm/s cannot be produced by the onset of diffusive motions of the whole bacteria. Such diffusive motions should have the same effect on the shape of the spectra corresponding to all iron within the cell. The fact that the Fe^{2+} spectrum above 270 K is narrow and well defined proves that the effect of the diffusive motions of the whole bacteria on the shape of the broad spectrum is extremely small. The

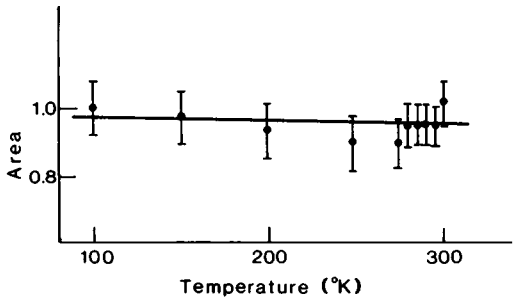

FIGURE 4 The total area of the Mössbauer spectrum as function of temperature.

broadening produced by the whole cell diffusive motions is expected to be <0.5 mm/s because of the large size of the cells (~3 μm) and the large effective viscosity in the packed cell sample.

The striking spectral change at 270 K can be explained by the onset of diffusive motions of the Fe_3O_4 particles in the bacteria as they are warmed through the solid-liquid phase transition of the cytoplasmic fluid at 270 K. Evidence for this comes from the fact that for freeze-dried cells (2, 4) the sharp-line spectrum persists at 300 K and the broad-line spectrum is never observed. Below we present an analysis of the broad-line spectra based on an extension of the "bounded diffusion" model previously developed for iron-containing proteins in the whole cells (7, 9, 10). The theory is presented below. From the analysis we derive the diffusion constant D of the magnetosomes, the effective viscosity η of the magnetosome environment, and a limit for the mean-squared translational displacement $\langle x^2 \rangle$ and rotational displacement $\langle \theta^2 \rangle$ of the magnetosomes as a function of temperature.

THEORY

The Extended Bounded Diffusion Model

A full calculation of the Mössbauer absorption spectra of overdamped harmonically bound particles in translational Brownian motion is given in references 9 and 10. We derive here an extension of this model for rigid spherical particles of radius R participating in both translational and rotational diffusive motions. As we do not know the exact restoring moments acting on the magnetosomes in the bacteria, we estimate the maximum contribution of the rotational diffusion to the line width. The maximum contribution will be obtained in the case of the free rotational diffusion in a viscous medium neglecting restoring moments.

Pure Translation Diffusion. The Brownian translational motion in one dimension of a particle of mass m which is bound to a center by a harmonic force $-mw^2x$, damped by a frictional force $-m\beta\, dx/dt$, and acted upon by random forces $F(t)$ has been treated in a classic paper by Uhlenbeck and Ornstein (11). In that paper, the classical self-correlation function $G(x, x_0, t)$ of the motion is derived in terms of two parameters, the diffusion constant D given by $k_B T/m\beta$ and the ratio between the harmonic and frictional force constants $\alpha = w^2/\beta$. Equipartition of energy gives

$$\langle x^2 \rangle = \frac{k_B T}{mw^2} = D/\alpha. \tag{1}$$

The pure translational Brownian motion in three dimensions of a particle in the overdamped case ($w \ll \beta$), will yield a Mössbauer spectrum (10) given by

$$I(\omega) = \frac{1}{2\pi}\int_{-\infty}^{\infty} dt \exp\left[-i(\omega-\omega_0)t - \frac{\Gamma}{2}|t| - \frac{k^2 D}{\alpha}(1 - e^{-\alpha|t|})\right] \tag{2}$$

where Γ is the natural line width of the γ-ray (0.1 mm/s) and k is the wave number of the γ-ray. Eq. 2 can also be expressed as the sum of a narrow line with natural line width and an infinite sum of Lorentzian lines (12). Expanding $\exp(k^2 \langle x^2 \rangle e^{-\alpha t})$ in series yields

$$I(\omega) = \exp(-k^2\langle x^2\rangle)\frac{\Gamma/2\pi}{(\Gamma/2)^2 + (\omega-\omega_0)^2} + \sum_{n=1}^{\infty}\frac{1}{\pi}\exp(-k^2\langle x^2\rangle)\frac{(k^2\langle x^2\rangle)^n}{n!} \cdot \frac{\Gamma/2 + n\alpha}{(\Gamma/2 + n\alpha)^2 + (\omega-\omega_0)^2}. \tag{3}$$

The relative intensity of the narrow line is given by $e^{-k^2\langle x^2\rangle}$. The sum of the broad Lorentzian lines can be approximated by a single Lorentzian line, the width of which (in units of α) is shown in Fig. 5 as a function of $k^2\langle x^2\rangle$. For $(k^2\langle x^2\rangle) < 0.1$, the intensity of the wide line will be <10%. For $(k^2\langle x^2\rangle) > 4$, where the relative intensity of the narrow line is negligible, the half-line width of the wide line is approximately $k^2\alpha\langle x^2\rangle = k^2 D$, where D is the

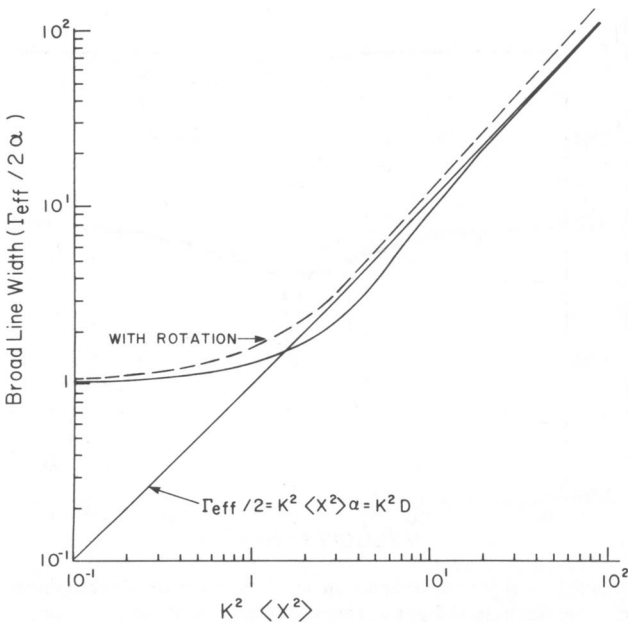

FIGURE 5 The theoretical width of the wide line (in units 2α) as function of $k^2\langle x^2\rangle$. The solid curve line corresponds to pure bound translational diffusion. The dashed line corresponds to a combination of bound translational diffusion with free rotational diffusion. The straight line corresponds to a line width of $2k^2D$ (width obtained in the case of free diffusion).

translational diffusion constant $D = k_B T/6\pi R\eta$. R is the radius of the spherical particles and η is the viscosity of the medium. This width is also obtained in the case of free translational diffusion (13). The total width in energy units is $2\hbar k^2 D$ ergs.

Rotational Diffusion of a Sphere Neglecting Restoring Moments. Free rotational diffusion (with no translational diffusion and no restoring moments) also leads to a spectrum which is a sum of Lorentzian lines (14). The contribution to the Mössbauer spectrum from a rotating nucleus at distance r from the center of the sphere is

$$I_r(\omega) = j_0^2(kr)\frac{\Gamma/2\pi}{(\Gamma/2)^2 + (\omega - \omega_0)^2} + \sum_{l=1}^{\infty}\frac{(2l+1)j_l^2(kr)(\Gamma/2 + l(l+1)D_r)}{(\Gamma/2 + l(l+1)D_r)^2 + (\omega - \omega_0)^2}. \quad (4)$$

Here $j_l(kr)$ are the spherical Bessel functions and D_r is the rotational diffusion constant $D_r = k_B T/8\pi R^3\eta$. For a sphere of radius R,

$$D_r = 0.75 \cdot D/R^2. \quad (5)$$

The Mössbauer spectrum obtained from the whole rotating sphere will be given by

$$I(\omega) = \frac{3}{R^3}\int_0^R I_r(\omega) r^2 dr. \quad (6)$$

The spectrum includes a line with natural line width whose relative intensity is given by

$$\frac{3}{R^3}\int_0^R j_0^2(kr) r^2 dr = \frac{3}{2}\left(kR - \frac{1}{2}\sin 2kR\right)\Big/(kR)^3. \quad (7)$$

In our case, where $R \sim 200$ Å, and $k = 7.3$ Å^{-1} (for the 14.4 keV γ-ray of Fe^{57}) the relative intensity of the narrow line is $<10^{-6}$. The sum of the broad lines can be approximated by a single broad Lorentzian lines.

Combination of Translational Diffusion and Free Rotational Diffusion. For particles in a sphere, participating in both bound-translational and free-rotational diffusive motions (without restoring moments), the two forms of motion are uncorrelated and the "intermediate scattering function" (15) can be expressed as the product of the translational diffusion function

$$F_{tr}(k, t) = \{\exp[-k^2\langle x^2\rangle(1 - e^{-\alpha t})]\} \quad (8)$$

and the rotational diffusion function (14)

$$F_{rot}(r, k, t) = \sum_{l=0}^{\infty}(2l+1) j_l^2(kr)\exp[-l(l+1)D_r t]. \quad (8a)$$

The average spectrum for all nuclei in the sphere is now given by

$$I(\omega) = \frac{3}{R^3}\int_0^R r^2 dr \frac{1}{2\pi}\int_{-\infty}^{\infty} \cdot \exp\left[-i(\omega - \omega_0)t - \frac{\Gamma}{2}|t|\right] \cdot F_{tr}(k, t) F_{rot}(r, k, t) dt. \quad (9)$$

$I(\omega)$ can be expressed as a double infinite sum of Lorentzian lines;

$$I(\omega) = \sum_{n=0}^{\infty}\sum_{l=0}^{\infty}\frac{A_{nl}\Gamma_{nl}/2\pi}{(\Gamma_{nl}/2)^2 + (\omega - \omega_0)^2} \quad (10)$$

where $\Gamma_{nl}/2 = (\Gamma/2) + n\alpha + l(l+1)D_r$ and

$$A_{nl} = \exp(-k^2\langle x^2\rangle)\frac{(k^2\langle x^2\rangle)^n}{n!}(2l+1)\frac{3}{R^3}\int_0^R j_l^2(kr) r^2 dr.$$

The value of the last integral is given by

$$\int_0^R j_l^2(kr) r^2 dr = (R^3/2)[j_l^2(kR) + j_{l-1}^2(kR) - (2l+1) j_l(kR) j_{l-1}(kR)/kR]. \quad (11)$$

For a sphere of radius R, D_r is given in Eq. 5, and the values of $\Gamma_{nl}/2$ are given by

$$\Gamma_{nl}/2 = \Gamma/2 + \alpha[n + 0.75l(l+1)k^2\langle x^2\rangle/k^2R^2]. \quad (12)$$

The Mössbauer spectrum given by Eq. 10 is composed of a relatively narrow subspectrum corresponding to $n = 0$ and a broad spectrum corresponding to $n \geq 1$. The relative intensity of the $n = 0$ subspectrum is $\exp(-k^2\langle x^2\rangle)$. We approximate each subspectrum by an effective Lorentzian line with a width given by the harmonic average of the Lorentzian lines of the subspectrum.

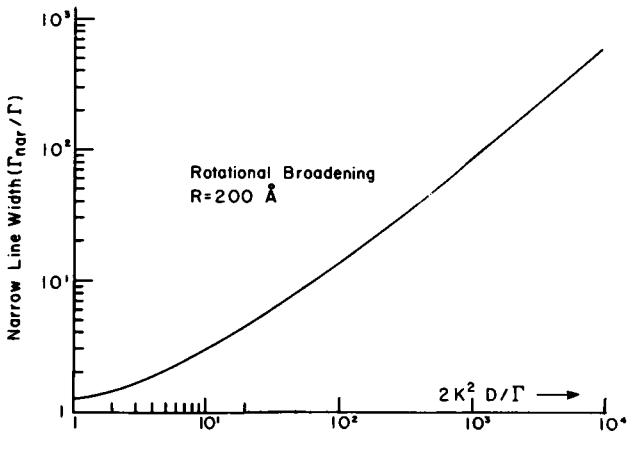

FIGURE 6 The width of the $n = 0$ subspectrum Γ_{nar}, in units of Γ (the natural width of the Mössbauer absorption line, ~0.1 mm/s) as function of $2k^2D/\Gamma$ for spheres of a radius of 200 Å participating in bounded translational diffusive motions and in free (no restoring moments) rotational diffusive motions (see Eq. 13).

The width of the $n = 0$ subspectrum is given by

$$\frac{1}{\Gamma_{nar}} = \exp(k^2\langle x^2\rangle)\sum_{l=0}^{\infty}\frac{A_{0l}}{\Gamma_{0l}} = \frac{\exp(k^2\langle x^2\rangle)}{\Gamma}\sum_{l=0}^{\infty}\cdot\frac{A_{0l}}{1+0.75l(l+1)\frac{2k^2D}{\Gamma}}. \quad (13)$$

This width Γ_{nar} is a function of R and $2k^2D/\Gamma$. Assuming that $R = 200$ Å, the values of Γ_{nar} as a function of $2k^2D/\Gamma$ were calculated and are shown in Fig. 6.

Similarly, the effective width of the broad line corresponding to $n \geq 1$ is given by

$$\frac{1}{\Gamma_{eff}} = \frac{\exp(k^2\langle x^2\rangle)}{\exp(k^2\langle x^2\rangle) - 1}\sum_{n=1}^{\infty}\sum_{l=0}^{\infty}\frac{A_{nl}}{\Gamma_{nl}}. \quad (14)$$

The values of $\Gamma_{eff}/2\alpha$ for $R = 200$ Å were calculated as a function of $k^2\langle x^2\rangle$ and are shown in Fig. 5 (dashed line). When $(k^2\langle x^2\rangle) > 4$, the relative intensity of the narrow line is negligible. The rotational diffusive motions contribute to the width of the broad line, and the total width of the broad line is larger than $2k^2D$. The width of the broad line depends on the radius of the spheres participating in the diffusive motions. In Fig. 7 the width of the broad line in units of $2k^2D$ is plotted as a function of k^2R^2, [for $(k^2\langle x^2\rangle) > 4$]. For $k^2R^2 > 10$, the ratio $\Gamma_{eff}/2k^2D$ reaches a saturation value of 1.271. For $R = 200$ Å, $k^2R^2 = 2 \cdot 10^6$ and the width of the broad line is $2 \cdot 1.271\ k^2D$.

The calculations lead to the conclusion that for a sphere with $R = 200$ Å, and $(k^2\langle x^2\rangle) > 4$, the spectrum consists only of a broad line, the width of which is given by $2\sigma k^2D$, where $1 < \sigma < 1.27$. σ is closer to 1.0 when the rotational diffusive motions are small and may be neglected. σ is close to 1.27 when the rotational diffusion may be regarded as "free" (restoring moments may be neglected).

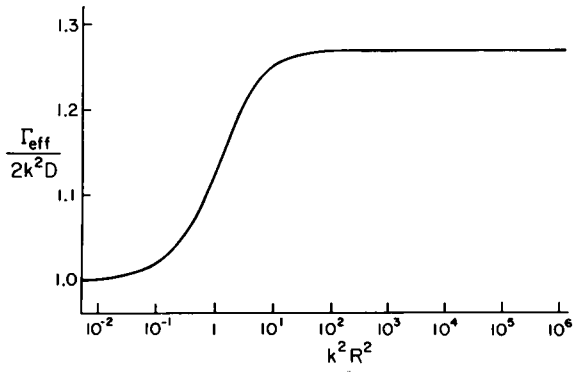

FIGURE 7 The width of the broad line ($n \geq 1$) in units of $2k^2D$ as function of k^2R^2 for a sphere of radius R participating in both translational and free rotational diffusion, assuming that $k^2(\langle x^2\rangle) > 4$.

ANALYSIS OF EXPERIMENTAL RESULTS AND DISCUSSION

We analyze the experimental results using the extended bounded diffusion model described above, assuming that the magnetic particles are spheres of radius 230 Å. We do not make any assumptions about the strength of the restoring forces and moments. We treat the motions in the overdamped limit, since according to the theory, the experimentally observed broad Lorentzian lines are only obtained in the overdampled limit. We carry out the analysis for two extreme possibilities: (*a*) pure translational diffusion, without rotational diffusion; and (*b*) translational diffusion with free rotational diffusion (neglecting restoring moments).

(*a*) For pure translational diffusion, the relative intensity of the narrow line is given by $\exp(-k^2\langle x^2\rangle)$. In the experimental spectra above 275 K, this intensity is >0.2%, thus yielding $(k^2\langle x^2\rangle) > 6$. We see from the graph in Fig. 5, corresponding to pure translation motions, that for $(k^2\langle x^2\rangle) > 6$, $\Gamma_{eff} = (0.9 \pm 0.1) \cdot 2\ k^2D$.

(*b*) In the case of translational diffusion with free rotational diffusion, one could try the assumption that the observed broad line is the line corresponding to $n = 0$ (Eq. 13) and that the line corresponding to $n > 1$ (Eq. 14) is weak and very broad and is, therefore, not observed experimentally. The meaning of such an assumption is that the particle is very strongly bound as far as translational motions are concerned, but is free to rotate in the viscous medium, which is extremely unlikely. The observed broad spectrum must, therefore, include both the $n = 0$ and the $n \geq 1$ lines. From Fig. 6 it follows that one of the following two relations always holds: (*a*) $\Gamma_{nar} < 80\ \Gamma$; or, (*b*) $\Gamma_{nar} < 10^{-1} \cdot 2k^2D$. According to Fig. 3, the experimental width W is larger than 800 Γ. From Fig. 5 it follows that $W > 2k^2D$. The conclusion is, therefore, that always $\Gamma_{nar} < 1/10W$. As the experimental spectra do not contain a narrow spectrum to within 10% in amplitude, the relative area of the narrow spectrum is <0.01, and the value of $k^2\langle x^2\rangle$ is, therefore, larger than 4.6. Using the graph corresponding to free rotation in Fig. 5, for values of $k^2\langle x^2\rangle$ larger than 4.6, we obtain the relation $\Gamma_{eff} = (1.17 \pm 0.10)\ 2k^2D$.

From the expressions obtained for the width of the broad spectrum in the two extreme cases (pure translational diffusion and translational diffusion with free rotational diffusion), we conclude that the expression for the total width of the spectra in the case of a combination of translational diffusion with any rotational diffusion is $\Gamma_{eff} = (1.03 \pm 0.23)\ 2k^2D$. Using this expression for Γ_{eff}, the diffusion constants of the magnetic particles are calculated from the experimental values of the line widths given in Fig. 3. D changes between $(50 \pm 12) \cdot 10^{-10}$ cm²/s at 270 K to $(96 \pm 22) \cdot 10^{-10}$ cm²/s at 295 K. The effective viscosity η of the medium surrounding the magnetic particles is calculated using the formula $D = kT/6\pi R\eta$, taking

R as 230 Å (6). The value of η as a function of temperature is shown in Fig. 8. η changes from 17 cP at 270 K to 10 cP at 295 K. We estimate that the errors in the absolute values of η are ~30%. The errors on the relative values of η as a function of temperature are ~5%. The viscosity of water as a function of temperature is also shown in Fig. 8. The effective viscosity of the medium surrounding the magnetosomes is thus ~15 times greater than the viscosity of water but its temperature dependence is quite similar to that of water.

As seen from Fig. 4, the areas of the absorption spectra above 270 K are equal, to within 5%, to the areas below 270 K. This proves that the spectra observed experimentally above 270 K are the whole spectra at these temperatures. The magnetic particles do not participate in motions additional to those which are responsible for the spectra observed in the velocity range between −150 mm/s and +150 mm/s.

The cytoplasm of a bacterium is probably not a homogeneous medium. The effective viscosities determined in the present work are the average viscosities of the materials surrounding the magnetic particles. A comparison of the present result with those obtained previously by measuring rotational correlation times for tempone in the cytoplasm of *E. coli* bacteria (16) shows that the effective viscosity in the magnetic bacteria is larger by a factor of 2 than in *E. coli*.

We now estimate the size of the displacements of a magnetic particle from its equilibrium position, as a result of its diffusive motions. We have already concluded from the experimental values of the upper limit of the relative intensity of the narrow spectrum that $(k^2\ \langle x^2\rangle) > 4.6$. Using the value $k^2 = 53 \cdot 10^{16}\ \text{cm}^{-2}$, we find that $(\langle x^2\rangle) > 0.12\ \text{Å}^2$. ($\langle x^2\rangle$ is the mean square translational deviation in the x direction; $\langle r^2\rangle$, the total mean square translational deviation, is equal to $3\langle x^2\rangle$; $\langle r^2\rangle$ is, therefore, larger than 0.36 Å^2.) If we only take into account restoring forces and restoring moments produced by the magnetic interactions, then the energy of a magnetic particle is approximately given by

$$E \approx (-4M^2/d^3)(1 - 0.5\,\theta^2 - 1.5\,x^2/d^2) \qquad (15)$$

where M is the magnetic moment of each magnetic particle, d is the distance between the centers of adjacent particles, x is the displacement of the particle in a direction perpendicular to the chain of magnetic particles, and θ is the rotation around an axis perpendicular to the chain. Eq. 15 is obtained by treating each magnetic particle as a magnetic dipole located at the center of the particle and having a magnetic moment M. In our case $M = 4 \cdot 10^{-14}$ emu (particle dimension is 220 Å and the saturation magnetization of bulk Fe_3O_4 is 480 G/cm^3) and $d = 500$ Å. Thus, $m = 12\,M^2/d^5 = 6$ erg/cm^2. Equipartition of energy gives $\langle x^2\rangle = k_BT/m = 70$ Å^2. If additional restoring forces exist then $\langle x^2\rangle < 70$ Å^2. The conclusion is, therefore, that $0.12\ \text{Å}^2 < (\langle x^2\rangle) < 70\ \text{Å}^2$ or $0.35\ \text{Å} < [\langle x^2\rangle]^{1/2} < 8.4$ Å.

From Eq. 15 the restoring moment constant C is equal to $4M^2/d^3 = 0.5 \cdot 10^{-10}$ erg. Equipartition of energy gives $\langle\theta^2\rangle < k_BT/C$. Thus $\langle\theta^2\rangle < 8.4 \cdot 10^{-4}$ or $[\langle\theta^2\rangle]^{1/2} < 0.029$ rad, which means that diffusive rotations are < 1.5°. The upper limit for the displacements due to rotational diffusion is $(a/2)[\langle\theta^2\rangle]^{1/2} = 6$ Å ($a = 420$ Å is the dimension of the particle). The small value of $\langle x^2\rangle^{1/2}$ and $\langle\theta^2\rangle^{1/2}$ imply that the particles are fixed relative to each other in the cell.

The fact that the additional Fe^{3+} quadrupole doublet in the spectrum broadened together with the Fe_3O_4 lines is consistent with previous cell fractionation studies (4). The Fe^{3+} in the cell has been characterized as a hydrous-ferric-oxide precursor to Fe_3O_4 precipitation that is physically associated with the magnetosomes. Hence this material would participate in the diffusive motions of the magnetosomes and a broad line spectrum is expected. Because of the relatively low intensity of the quadrupole doublet, its wide-line spectrum is buried in the Fe_3O_4 wide-line spectrum.

The fact that the sharp-line Fe^{2+} spectrum remains even when the Fe_3O_4 lines have broadened shows that the Fe^{2+} material is not associated with the magnetosomes. (Fe^{2+} in the cells is thought to result from reduction of chelated Fe^{3+} which the cells take up from the external medium [4]. The Fe^{2+} is subsequently reoxidized and deposited as hydrous-ferric-oxide.) As noted above, in wet, packed cells held anaerobically above freezing temperature, degradative processes reduce the hydrous-ferric-oxide to Fe^{2+}. If the Fe^{2+} remained associated with the magnetosomes, or if the Fe^{2+} was dissolved in the cytoplasm, diffusive motion would broaden the sharp-line spectrum at $T > 275$ K, contrary to experiment. This suggests that the Fe^{2+} is not associated either with the magnetosomes or with the cytoplasm in the cells. The Fe^{2+} is very probably associated with the cell wall. Metal ions are bound by the cell wall (17) and peptidoglycan (18) in some gram-positive bacte-

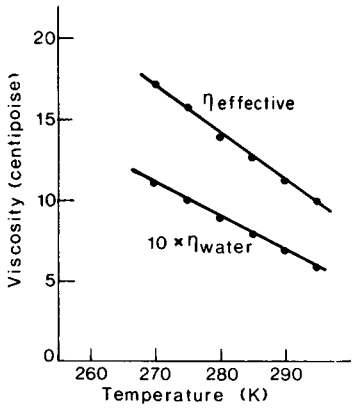

FIGURE 8 The viscosity of the medium surrounding the magnetic particles as function of temperature. The viscosity of water is shown in the graph on an extended scale.

ria. On the other hand, heavy metals are accumulated intracellularly in gram-negative species (19). In gram-negative *A. magnetotacticum*, ferrous iron could be transiently associated with the cell envelope during its conversion from the iron quinate complex outside the cell to ferric iron and ultimately Fe_3O_4 within the cell.

We thank Dr. F. F. Torres de Araujo for participation in the early phases of this study and Dr. S. G. Cohen for discussion of the results.

Drs. Ofer, Nowik, and Bauminger were partially supported by the Stiftung Volkswagenwerk. Drs. Papaefthymiou and Frankel were partially supported by the Office of Naval Research. Dr. Blakemore was supported by the Office of Naval Research and the National Science Foundation. The Francis Bitter National Magnet Laboratory is supported by the National Science Foundation.

Received for publication 15 September 1983 and in final form 5 March 1984.

REFERENCES

1. Blakemore, R. P., D. Maratea, and R. S. Wolfe. 1979. Isolation and pure culture of a freshwater magnetic spirillum in chemically defined medium. *J. Bacteriol.* 140:720–729.
2. Frankel, R. B., R. P. Blakemore, and R. S. Wolfe. 1979. Magnetite in freshwater magnetotactic bacteria. *Science (Wash. DC).* 203:1355–1356.
3. Balkwill, D. L., D. Maratea, and R. P. Blakemore. 1980. Ultrastructure of a magnetotactic spirillum. *J. Bacteriol.* 141:1399–1408.
4. Frankel, R. B., G. C. Papaefthymiou, R. P. Blakemore, and W. O'Brien. 1983. Fe_3O_4 precipitation in magnetotactic bacteria. *Biochim. Biophys. Acta.* 763:147–159.
5. Frankel, R. B., and R. P. Blakemore. 1980. Navigational compass in magnetic bacteria. *J. Magn. Mater.* 15–18:1562–1564.
6. Craig, P. P., and N. Sutin. 1963. Mössbauer effect in liquids: influence of diffusion broadening. *Phys. Rev. Lett.* 11:460–462.
7. Bauminger, E. R., S. G. Cohen, S. Ofer, and U. Bachrach. 1982. Study of storage iron in cultured chick embryo fibroblasts and rat glimoa cells, using Mössbauer spectroscopy. *Biochim. Biophys. Acta.* 720:133–140.
8. Maratea, D., and R. P. Blakemore. 1981. *Aquaspirillum magnetotacticum* sp. nov., a magnetic spirillum. *Int. J. Syst. Bacteriol.* 31:452–455.
9. Bauminger, E. R., S. G. Cohen, I. Nowik, S. Ofer, and J. Yariv. 1983. Dynamics of heme iron in crystals of metmyoglobin and deoxymyoglobin. *Proc. Natl. Acad. Sci. USA.* 80:736–740.
10. Nowik, I., S. G. Cohen, E. R. Bauminger, and S. Ofer. 1983. Mössbauer absorption in overdamped harmonically bound particles in Brownian motion. *Phys. Rev. Lett.* 50:1528–1530.
11. Uhlenbeck, G. E., and L. S. Ornstein. 1930. On the theory of the Brownian motion. *Phys. Rev.* 36:823–841.
12. Parak, F., E. W. Knapp, and D. Kucheida. 1982. Protein dynamics. Mössbauer spectroscopy on deoxymyoglobin crystals. *J. Mol. Biol.* 161:177–194.
13. Singwi, K. S., and A. Sjolander. 1960. Resonance absorption of nuclear gamma rays and the dynamics of atomic motions. *Phys. Rev.* 120:1093–1102.
14. Springer, T. 1972. Quasielastic neutron scattering for the investigation of diffusive motions in solids and liquids. *In* Springer Tracts in Modern Physics. G. Höhle, editor. Springer-Verlag, Berlin. 63:67.
15. van Hove, L., 1954. Correlations in space and time and Born approximation scattering in systems of interacting particles. *Phys. Rev.* 95:249–262.
16. Keith, A. D., and W. Snipes. 1974. Viscosity of cellular protoplasm. *Science (Wash. DC).* 183:666–668.
17. Beveridge, T. J., C. W. Forsberg, and R. J. Doyle. 1982. Major sites of metal binding in *Bacillus licheniformis* walls. *J. Bacteriol.* 150:1438–1448.
18. Beveridge, T. J., and R. G. E. Murray. 1976. Uptake and retention of metals by cell walls of *Bacillus subtilis*. *J. Bacteriol.* 127:1502–1518.
19. Strandberg, G. W., S. E. Shumate, III, and J. R. Parrott, Jr. 1981. Microbial cells as biosorbants for heavy metals: accumulation of uranium by *Saccharomyces cerevesiae* and *Pseudomonas aeruginosa*. *Appl. Environ. Microbiol.* 41:237–245.